



Effects of capping layers on the photoelectrochemical property of silver nanoparticle-modified indium–tin-oxide electrode

Ken-ichi Matsuoka^a, Hironobu Tahara^a, Tsuyoshi Akiyama^{a,b}, Sunao Yamada^{a,b,*}

^a Department of Materials Physics and Chemistry, Graduate School of Engineering, Kyushu University, 744 Motoooka, Nishi-ku, Fukuoka 819-0395, Japan

^b Department of Applied Chemistry, Faculty of Engineering, Kyushu University, 744 Motoooka, Nishi-ku, Fukuoka 819-0395, Japan

ARTICLE INFO

Article history:

Available online 25 March 2011

Keywords:

Silver nanoparticles
Photocurrent
Plasmon band
Photoelectrochemistry

ABSTRACT

Photoelectrochemical properties of indium–tin-oxide (ITO) substrate modified with silver nanoparticles (AgNPs) and effects of surface capping layer of AgNP were investigated in the water/acetonitrile (H₂O/MeCN) electrolyte solutions with the presence of oxygen as an electron acceptor. The modified ITO substrate showed photocurrent response mainly driven by the photoinduced electron transfer from ITO substrate to AgNPs. In addition, its photoelectrochemical property significantly depended on the solvent composition of electrolyte solution which was in correlation with surface status of AgNPs. Combination of photoelectrochemical measurements and spectroscopic analysis suggested that presence of considerable amount of MeCN in the electrolyte solution triggered partial displacement of capping citrate ions to activate photocurrent generation.

© 2011 Elsevier B.V. All rights reserved.

1. Introduction

Understanding of photoelectrochemical processes between semiconductor and metal nanoparticle (MNP) is one of the central issues in the range of photocatalytic and photovoltaic applications [1–5]. To date, photoelectrochemical properties of several semiconductor–MNP composite systems, such as ZnO–MNP [1,2] and TiO₂–MNP [3–5], have been investigated to evaluate their peculiar photoelectric interactions and potential utilities in related device performance.

Photoelectrochemical interaction between indium and tin-oxide (ITO) and MNP is a particular interest since ITO is one of the versatile semiconducting materials and offers highly conductive and transparent supports for the various MNP-based photoelectrochemical architectures [6–10]. In particular, our group recently reported that AuNP [6,7] and AgNP [8] arrays deposited on ITO substrate substantially enhanced photocurrent signals from attached organic dyes due to the electric field generated by the localized surface plasmon (LSP) excitation.

In such systems, LSP-assisted excitation of organic dyes have been the main focus, but other potential factors for the overall photoelectrochemical outputs, such as photoinduced interactions between the substrate and MNPs, have not been carefully examined. Along with this line, clarification of the photoelectric

interaction between ITO substrate and MNPs will offer an additional basis for the development of photoactive nanostructures to utilize unique optical and electrochemical properties of MNPs. These circumstances encouraged us to investigate the photoelectrochemical properties of ITO substrates modified with AuNP and AgNP arrays [11,12]. However, clarification of such photoelectrochemical systems has not been accomplished yet.

We report herein the preliminary investigation of the photoelectrochemical property involving AgNP and ITO substrate with an emphasis on the effect of capping layers of AgNP. The emphasis was made as considering the fact that capping layers on MNPs regulate wide range of physical aspects such as optical [13], conductive [14], catalytic [15], electrochemical [16], and photoelectrochemical [17] properties. In this study, photoinduced electron transfer in ITO–AgNP system and deep correlation between the surface status of AgNPs and the photoelectrochemical performance of AgNP-deposited ITO substrate were evaluated.

2. Experimental

2.1. Materials

Silver nitrate (AgNO₃, 99.5%, Wako), trisodium citrate dehydrate (99%, Wako), sodium tetrahydroborate (NaBH₄, 97%, Kishida), sodium chloride (NaCl, 99.5%, Wako), poly(ethyleneimine) (PEI, M_w = 50,000–100,000, Wako), sodium perchlorate (NaClO₄, 95%, Wako), acetonitrile (MeCN, 99.5%, Wako), 1-octadecanethiol (ODT ≥ 90%, wako), and hydroxyethanethiol (95%, Wako) were used

* Corresponding author at: Graduate School of Engineering, Kyushu University, Japan.

E-mail address: yamada@mail.cstm.kyushu-u.ac.jp (S. Yamada).

as received. Pure water (18 M Ω cm) was obtained from Mill-Q Academic A-10 system (Millipore).

2.2. Preparation of AgNPs

Citrate-capped AgNPs were synthesized by the modified method of Wang et al. [18]. Briefly, an aqueous solution of 0.5 mM AgNO₃ (100 ml) was added into the equivalent volume of aqueous solution containing 2 mM of NaBH₄ and 0.13 mM of trisodium citrate under the cooling in ice-bath, forming a yellowish colloidal solution of AgNPs. The colloidal solution was heated to 70 °C to decompose excess NaBH₄, and then cooled to room temperature. The average diameter of resultant AgNPs was evaluated to be 13.5 \pm 3.3 nm from the transmission electron microscope (TEM) images (Fig. S1).

2.3. Fabrication of AgNP-modified ITO substrate

The ozone-cleaned ITO substrate (200 nm thickness of ITO film deposited on the glass substrate, Geomatec Co. Ltd., 10 Ω /square) was immersed into an aqueous solution of PEI (45 mg/ml) containing 0.2 M NaCl for 10 min at 30 °C. After withdrawal, the substrate was washed with H₂O under sonication. The resultant PEI-coated ITO substrate is denoted as ITO/PEI. The AgNP-modified ITO substrate, denoted as ITO/PEI/AgNP, was obtained by soaking ITO/PEI into the colloidal solution of AgNPs for 12 h at room temperature, followed by rinsing with water.

2.4. Measurements

UV–vis spectral measurements were carried out by JASCO V-670 spectrophotometer. Transmittance–reflectance spectral measurements were carried out by Shimadzu UV-3150 spectrophotometer. Scanning electron microscope (SEM) images were taken on Hitachi S-5000 electron microscope with an acceleration voltage of 10 kV. TEM images were taken on JEOL JEM-2010 electron microscope with an acceleration voltage of 120 kV. Quartz crystal microbalance (QCM) measurements were performed with ALS Model 420 Electrochemical analyzer. Gold-covered QCM plates (8 MHz) were used for QCM measurements in order to estimate the thickness of PEI film. Namely, the QCM plate was immersed in an ethanol solution of 1 mM hydroxyethanethiol for one day to implant hydroxyl groups on the surface of QCM plate prior to PEI coating [12]. Photocurrent measurements of ITO/PEI/AgNP (working) were carried out by the three-electrode photoelectrochemical cell using a Ag/AgCl (sat. KCl) electrode (reference) and a platinum coil (counter). Oxygen bubbling was carried out for 60 min prior to the measurements. Monochromatic light from a Xe lamp irradiated the modified ITO substrate (irradiation area: 0.28 cm²) from the back side of the substrate, where AgNPs were not deposited, and the resultant photocurrents were measured with Huso HECS-318 C potentiostat. The irradiation power of the monochromatic light was determined by OPHIR power/energy meter NOVA.

3. Results and discussion

3.1. Characterization of ITO/PEI/AgNP substrate

Characterization of ITO/PEI/AgNP was carried out by UV–vis, SEM, and QCM measurements. Fig. 1b shows a typical UV–vis spectrum of ITO/PEI/AgNP. It exhibits broad bands around 420 and 580 nm, respectively. The former is mainly attributable to the plasmon band of isolated AgNPs, while the latter due to interparticle plasmon coupling of aggregated AgNPs. SEM image of ITO/PEI/AgNP (Fig. 1a) shows randomly deposited AgNP array (bright spots) on ITO/PEI. Presence of both isolated and aggregated AgNP was

confirmed. The surface coverage of AgNP was estimated to be $\sim 1.6 \times 10^{11}$ particles per 1 cm² from the SEM image, which corresponds to 22% of surface coverage based on the average diameter of AgNP. Thickness of PEI film was estimated from QCM measurements. Frequency decrease of 177 \pm 7 Hz was obtained upon PEI coating. This value corresponds to ca. 5.0 \pm 0.2 nm thickness of PEI film by assuming the reported density (1.2 g cm⁻³) [19].

3.2. Solvent-dependent stability and surface status of AgNP

Stability of AgNP array electrostatically deposited on ITO substrates was investigated in various H₂O/MeCN mixed solvents as a preparative step for photoelectrochemical measurements. Fig. 2 shows the time dependence of UV–vis spectral change of ITO/PEI/AgNP in H₂O/MeCN solutions with various volume ratios (H₂O/MeCN = 10/0–0/10; v/v) under aerated condition. As shown in Fig. 2a and b, no significant spectral changes were observed within the experimental period (120 min) when the volume fraction of MeCN was lower (H₂O/MeCN = 10/0, 9/1). Slight red-shift of spectrum is probably due to the local change of particle aggregation. In contrast, gradual decrease of plasmon band of AgNPs was observed when the volume fraction of MeCN was 30–50% (Fig. 2c and d). In addition, such spectral change became significant when the volume fraction of MeCN was larger than 70% (Fig. 2e and f). The degradation of plasmon band is attributable to the oxidation of AgNPs by oxygen. This was confirmed by the fact that purging the MeCN (H₂O/MeCN = 0/10) solution with nitrogen gas (15 min) prior to the UV–vis measurements effectively reduced the degradation of plasmon band (Fig. 2g) in comparison to the case under aerated condition (Fig. 2f).

Possible reason for the solvent-dependent oxidation of AgNP is partial displacement of citrate ions by MeCN present in the solution. It has been reported that MeCN molecules reversibly adsorb on the Ag surface through the interaction of nitrile group [20,21], where the activation energy of MeCN desorption, for example, was reported to be 10 kcal/mol at the (1 1 0) surface [20]. Adsorption of MeCN accompanies the removal of capping citrate ions. Thus, it is plausible that oxidation of AgNPs proceeds at the deprotected areas. Displacement of citrate ions must be accelerated by increasing the volume fraction of MeCN as can be recognized from Fig. 2a–f.

This assumption is further supported by the fact that the spectral degradation was remarkably suppressed by adding capping reagent (0.1 mM trisodium citrate) in the H₂O/MeCN = 3/7 solution (Fig. 2h), as compared with the case without trisodium citrate (Fig. 2e). In general, citrate ion is known as a capping reagent of metal colloids as well as a thermal reducing reagent [22]. However, reduction of Ag⁺ with citrate ion hardly proceeds at room temperature. Thus, these results suggest that the oxidation of AgNPs was mainly suppressed by securing the AgNP surface with citrate ions.

3.3. Photoelectrochemical property of ITO/PEI/AgNP and effect of surface status of AgNP

The photoelectrochemical property of ITO/PEI/AgNP was investigated in the 0.1 M NaClO₄ electrolyte solution using H₂O/MeCN mixed solvents (H₂O/MeCN = 10/0, 9/1, 7/3, 5/5; v/v) under oxygen-saturated condition. Photocurrent action spectra, except for ITO/PEI, were obtained by averaging the results of three independent samples.

Fig. 3 shows the relationship between photocurrent action spectra of the samples and electrolyte solution conditions. The photocurrents from ITO/PEI/AgNP were negligibly small when the volume fraction of MeCN was lower (H₂O/MeCN = 10/0, 9/1). On the contrary, distinct cathodic photocurrents were observed when the volume fraction was relatively higher (H₂O/MeCN = 7/3, 5/5). Remarkable photocurrent was observed up to around 450 nm

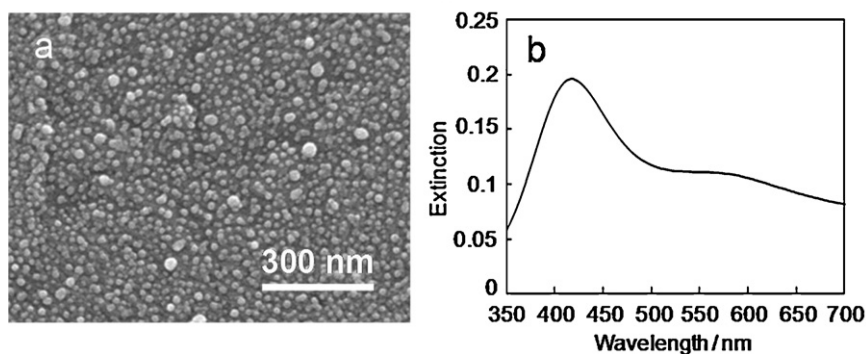


Fig. 1. (a) SEM image and (b) UV-vis spectrum of ITO/PEI/AgNP.

with a small peak at 380 nm. A control experiment without AgNP (ITO/PEI) in $\text{H}_2\text{O}/\text{MeCN} = 7/3$ showed negligible photocurrent response. It is notable that the sudden increase of the cathodic photocurrent signal and the degradation of the plasmon band of AgNP

(partial deprotection of citrate ions as described in Section 3.2) were observed at the same volume fraction of MeCN (30 vol.%). In addition, our previous studies showed that PEI film had no remarkable effects on the photoelectrochemical properties of the similar

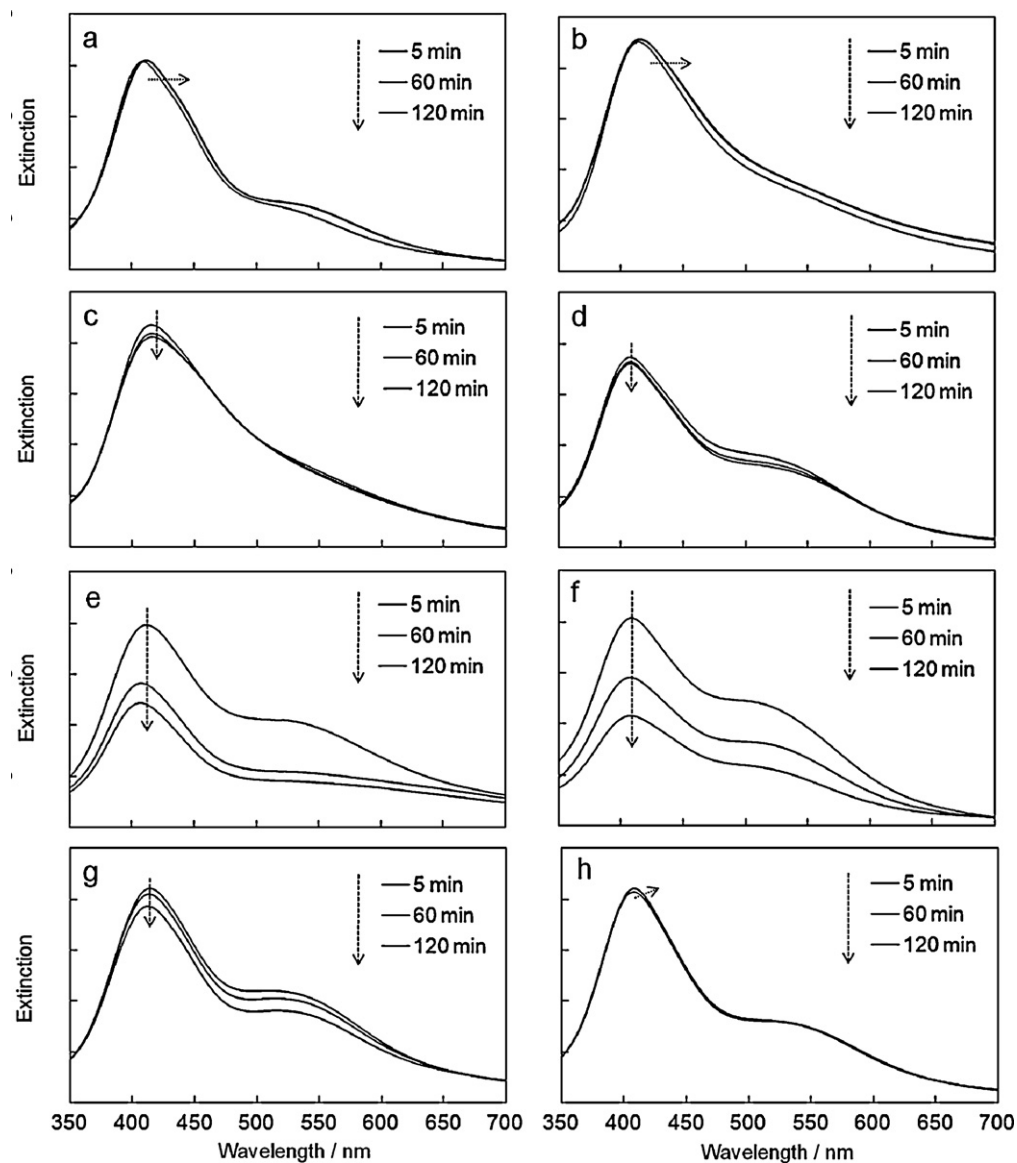


Fig. 2. Time-dependent change of UV-vis spectra of ITO/PEI/AgNP in air-saturated $\text{H}_2\text{O}/\text{MeCN}$ solutions with various volume ratios, unless otherwise noted. Volume ratios of $\text{H}_2\text{O}/\text{MeCN}$ are: (a) 10/0 (v/v), (b) 9/1 (v/v), (c) 7/3 (v/v), (d) 5/5 (v/v), (e) 3/7 (v/v), (f) 0/10 (v/v), (g) $\text{H}_2\text{O}/\text{MeCN} = 0/10$ with nitrogen bubbling (15 min) prior to measurement and (h) $\text{H}_2\text{O}/\text{MeCN} = 3/7$ with 0.1 mM trisodium citrate.

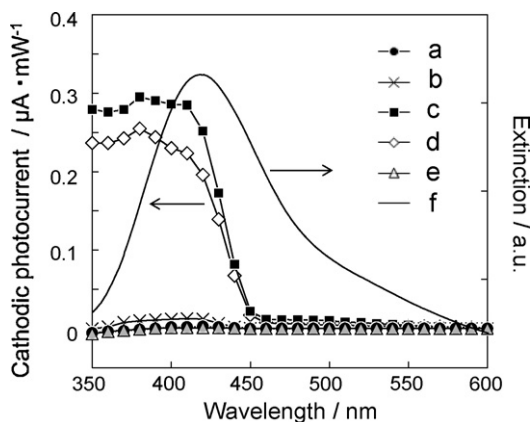


Fig. 3. Photocurrent action spectra of ITO/PEI/AgNP measured in oxygen-saturated H₂O/MeCN electrolyte solutions. Volume ratios of H₂O/MeCN are: (a) 10/0 (v/v), (b) 9/1 (v/v), (c) 7/3 (v/v) and (d) 5/5 (v/v). (e) Photocurrent action spectrum of ITO/PEI in oxygen-saturated H₂O/MeCN = 7/3 electrolyte solution. Applied potential $E = 0\text{ V}$ vs. Ag/AgCl (sat. KCl). (f) UV-vis spectrum of ITO/PEI/AgNP.

systems [7,8,11,12]. Therefore, it is strongly suggested that the photocurrent generation process involves partially deprotected AgNPs.

As shown in Fig. 3, photocurrent profiles of ITO/PEI/AgNP do not match the plasmon band of AgNPs. Therefore, we speculated that excitation of the ITO substrate is the major contribution of photocurrent. To verify this, the absorption profile of the ITO substrate was evaluated by transmittance–reflectance measurements. Absorption coefficient $\alpha(h\nu)$ of ITO was estimated by the following equation [23]:

$$\alpha(h\nu) = \frac{1}{l} \ln \frac{1 - R(h\nu)}{T(h\nu)} \quad (1)$$

where $R(\lambda)$ and $T(\lambda)$ correspond to reflectance and transmittance of ITO, respectively. l is the thickness of ITO film (200 nm in this study). The absorption coefficient can be described by the relation for parabolic bands as follows [24]:

$$(\alpha h\nu)^N \propto h\nu - E_g \quad (2)$$

where $h\nu$ represents the photon energy, E_g the optical band gap, and N depends on the type of electron transition: i.e. direct transition corresponds to $N=2$ and indirect transition correspond to $N=1/2$. As shown in Fig. 4a, we found a linear trend at higher photon energy region with an onset around 3.7 eV corresponding to the direct band gap energy under the condition of $N=2$. On the other hand, the indirect band gap energy of around 2.6 eV was also obtained in a similar manner from the analysis at $N=1/2$. These values are in agreement within the reported values [23,24].

Fig. 4b shows the absorption coefficient of the ITO substrate. In the present study, photocurrent generation becomes significant at the wavelength shorter than 450 nm (2.75 eV, see Fig. 3), which is

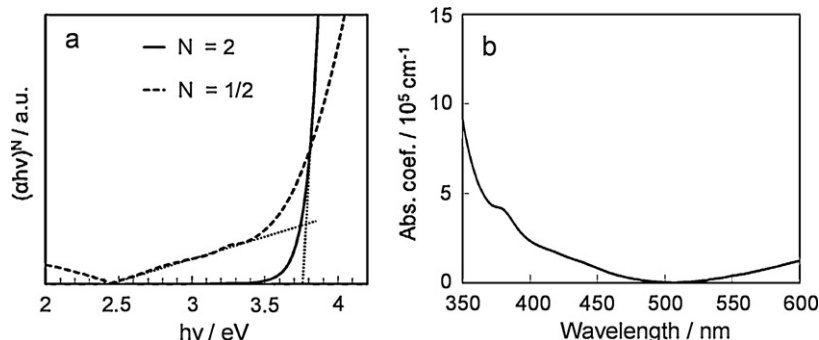


Fig. 4. (a) $(\alpha h\nu)^N$ vs. the photon energy ($N=2, 1/2$): solid line, $N=2$; dashed line, $N=1/2$ and (b) absorption coefficient of ITO substrate.

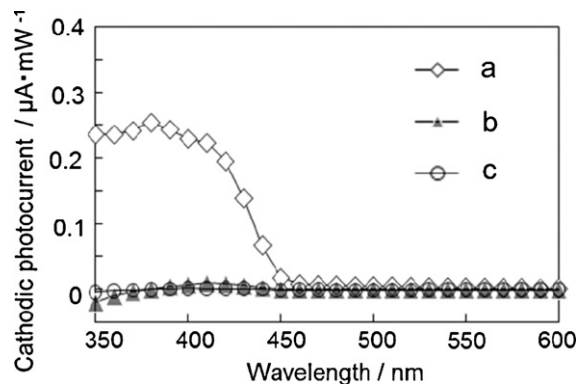


Fig. 5. Photocurrent action spectra of ITO/PEI/AgNP measured in oxygen-saturated H₂O/MeCN = 5/5 (v/v) solution: (a) without trisodium citrate, (b) with 0.1 mM trisodium citrate and (c) ODT-modified AgNP, without trisodium citrate. Applied potential $E = 0\text{ V}$ vs. Ag/AgCl (sat. KCl).

fairly correlated with the obtained indirect band gap energy 2.6 eV. Absorption at longer wavelength region ($>530\text{ nm}$) is ascribed to the plasma oscillation. In addition, ITO substrate has an absorption peak around 380 nm. This value matches well with the observed photocurrent peak at 380 nm (Fig. 3). These results imply that excitation of ITO substrate is the major contribution to the photocurrent generation.

It was expected that excited electrons in ITO substrate are first transferred to the attached AgNPs. Then, stored electrons in AgNPs participate in the reduction of oxygen to generate cathodic photocurrent. Solvent-dependent characteristics of photocurrent generation suggested that oxygen was dominantly reduced at the deprotected surface of AgNPs to generate cathodic photocurrent. It should be noted, however, that observed photocurrent profile and absorption profile of ITO substrate do not overlap completely. Photocurrent profile of ITO/PEI/AgNP showed shoulders around 410 nm while no such shoulder can be recognized in the absorption profile of ITO substrate. Since AgNP exhibited strong absorption close to the photocurrent shoulder with maximum around 420 nm, plasmon-excitation of AgNPs could also participate in the reduction of oxygen. Such phenomena have been observed in roughed Ag substrates under surface plasmon excitation [25]. Further studies are necessary to address this issue.

We also investigated the effect of the surface status of AgNPs on photocurrent generation by two experiments. First, photocurrent measurement was carried in the presence of 0.1 M trisodium citrate in the solution (H₂O/MeCN = 3/7). Second, AgNPs were modified with ODT by soaking ITO/PEI/AgNP in the ethanol solution containing 1 mM of ODT for one day. Then, the photocurrents of the ODT-modified sample were compared in the same electrolyte solution without trisodium citrate. Results of photocurrent measurements are shown in Fig. 5. Significant decrease of photocurrent

was also observed in both cases. As shown in Fig. 2h, presence of enough citrate ions in the surrounding medium effectively protects AgNP surface from oxygen. This is likely to inhibit the reduction process of oxygen upon the photoinduced electron injection from ITO to AgNPs. Surface-immobilized ODT layer also suppressed the reduction of oxygen at AgNP surface. Such barrier effect toward oxygen has been reported by Tatsuma and coworkers in AgNP/TiO₂ composite system [17]. These results further suggest the correlation between the surface status of AgNP and photoelectrochemical property of ITO/PEI/AgNP in the present experimental condition.

4. Conclusion

In summary, photoelectrochemical interaction between ITO substrate and AgNPs and the effect of surface status of AgNP on the photocurrent generation were investigated. Presence of photoinduced electron injection from the excited ITO substrate to AgNPs was strongly suggested by the analysis of the photocurrent profiles. Citrate ions and ODT capping layers on the AgNP surface exhibited barrier effect against oxygen. Meanwhile, MeCN removes some of the capping citrate ions from the AgNP surface, giving the photoelectrochemical activity to the system.

It was demonstrated that electrochemically negatively biased AuNP suppressed electron transfer process between AuNP and attached organic dye by repelling the electrons from excited dye [26]. Along with this line, photoinduced electron injection from excited ITO substrate to attached metal nanoparticles may be beneficial for dye-MNP composite photoelectrochemical systems to attain cathodic photocurrents by the suppression of unfavorable electron injection from excited dyes into MNPs to some extent. Basic understanding of photoelectrochemical interactions between conducting substrates and metal nanoparticles, as demonstrated a part in this study, will be an essential basics for the designing of MNP-based photoelectrochemical devices.

Acknowledgements

This research was partially supported by Research Fellowships of Japan Society for the Promotion of Science (JSPS) for young scientists (HAG1004391) and Grant-in-Aid for Scientific Research (No. 19201021) and of the Priority Area (Area code 470) from the Ministry of Education, Culture, Sports, Science and Technology (MEXT) of Japan.

Appendix A. Supplementary data

Supplementary data associated with this article can be found, in the online version, at doi:10.1016/j.jphotochem.2011.03.015.

References

- [1] A. Wood, M. Giersig, P. Mulvaney, Fermi level equilibration in quantum dot-metal nanojunctions, *J. Phys. Chem. B* 105 (2001) 8810–8815.
- [2] V. Subramanian, E.E. Wolf, P.V. Kamat, Green emission to probe photoinduced charging events in ZnO–Au nanoparticles. Charge distribution and Fermi-level equilibration, *J. Phys. Chem. B* 107 (2003) 7479–7485.
- [3] V. Subramanian, E.E. Wolf, P.V. Kamat, Catalysis with TiO₂/Gold nanocomposites. Effect of metal particle size on the Fermi level equilibration, *J. Am. Chem. Soc.* 126 (2004) 4943–4950.
- [4] T. Hirakawa, P.V. Kamat, Charge separation and catalytic activity of Ag@TiO₂ core-shell composite clusters under UV-irradiation, *J. Am. Chem. Soc.* 127 (2005) 3928–3934.
- [5] Y. Tian, T. Tatsuma, Mechanisms and applications of plasmon-induced charge separation at TiO₂ films loaded with gold nanoparticles, *J. Am. Chem. Soc.* 127 (2005) 7632–7637.
- [6] T. Akiyama, M. Nakada, N. Terasaki, S. Yamada, Photocurrent enhancement in a porphyrin-gold nanoparticle nanostructure assisted by localized plasmon excitation, *Chem. Commun.* (2006) 395–397.
- [7] K. Sugawa, T. Akiyama, H. Kawazumi, S. Yamada, Plasmon-enhanced photocurrent generation from self-assembled monolayers of phthalocyanine by using gold nanoparticle films, *Langmuir* 25 (2009) 3887–3893.
- [8] T. Arakawa, T. Akiyama, S. Yamada, Effect of silver nanoparticles on photoelectrochemical responses of organic dyes, *J. Phys. Chem. C* 113 (2009) 11830–11835.
- [9] M. Lahav, C.H. Shabtai, J. Wasserman, E. Katz, I. Willner, H. Durr, Y.-Z. Hu, S.H. Bossmann, Photoelectrochemistry with integrated photosensitizer–electron acceptor and Au-nanoparticle arrays, *J. Am. Chem. Soc.* 122 (2000) 11480–11487.
- [10] S. Yamada, T. Tasaki, T. Akiyama, N. Terasaki, S. Nitahara, Gold nanoparticle-porphyrin self-assembled multilayers for photoelectric conversion, *Thin Solid Films* 438–439 (2003) 70–74.
- [11] K. Sugawa, T. Kawahara, T. Akiyama, S. Yamada, Structural characterization and photoelectrochemical properties of gold nanoparticle multilayers prepared by layer-by-layer deposition, *Jpn. J. Appl. Phys.* 48 (2009) 04C132–5.
- [12] T. Arakawa, T. Akiyama, S. Yamada, Structural characterization and photoelectrochemical properties of silver nanoparticle-polyion films, *Trans. Mater. Res. Soc. Jpn.* 33 (2008) 185–188.
- [13] M.D. Malinsky, K.L. Kelly, G.C. Schatz, R.P. Van Duyne, Chain length dependence and sensing capabilities of the localized surface plasmon resonance of silver nanoparticles chemically modified with alkanethiol self-assembled monolayers, *J. Am. Chem. Soc.* 123 (2001) 1471–1482.
- [14] H. Ahn, A. Chandekar, B. Kang, C. Sung, J.E. Whitten, Electrical conductivity and vapor-sensing properties of ω-(3-thienyl)alkanethiol-protected gold nanoparticle films, *Chem. Mater.* 16 (2004) 3274–3278.
- [15] M.M. Maye, J. Luo, Y. Lin, M.H. Engelhard, M. Hapel, C.-J. Zhong, X-ray photoelectron spectroscopic study of the activation of molecularly-linked gold nanoparticle catalysts, *Langmuir* 19 (2003) 125–131.
- [16] S.W. Boettcher, S.A. Berg, M. Schierhorn, N.C. Strandwitz, M.C. Lonergan, G.D. Stucky, Ionic ligand mediated electrochemical charging of gold nanoparticle assemblies, *Nano Lett.* 8 (2008) 3404–3408.
- [17] K. Naoi, Y. Ohko, T. Tatsuma, Switchable rewritability of Ag–TiO₂ nanocomposite films with multicolor photochromism, *Chem. Commun.* (2005) 1288–1290.
- [18] W. Wang, S. Efrima, O. Regev, Directing oleate stabilized nanosized silver colloids into organic phases, *Langmuir* 14 (1998) 602–610.
- [19] T. Lvov, K. Ariga, M. Onda, I. Ichinose, T. Kunitake, A careful examination of the adsorption step in the alternate layer-by-layer assembly of linear polyanion and polycation, *Colloids Surf. A* 146 (1999) 337–346.
- [20] A.J. Capote, A.V. Hamza, N.D.S. Canning, R.J. Madix, The adsorption and reaction of acetonitrile on clean and oxygen covered Ag (1 1 0) surfaces, *Surf. Sci.* 175 (1986) 445–464.
- [21] L.M. Doubova, S. Trasatti, S. Valcher, Adsorption of acetonitrile on polycrystalline Ag electrodes: comparison with Hg electrodes, *J. Electroanal. Chem.* 349 (1993) 187–195.
- [22] J. Turkevich, P.C. Stevenson, J. Hiller, A study of the nucleation and growth processes in the synthesis of colloidal gold, *Discuss. Faraday Soc.* 11 (1951) 55–75.
- [23] F. Matino, L. Persano, V. Arima, D. Pisignano, R.I.R. Blyth, R. Cingolani, R. Rinaldi, Electronic structure of indium-tin-oxide films fabricated by reactive electron-beam deposition, *Phys. Rev. B* 72 (2005) 85437–85446.
- [24] J. Szczyrbowski, A. Dietrich, H. Hoffmann, Optical and electrical properties of RF-sputtered indium-tin oxide films, *Phys. Stat. Sol.* 78 (1983) 243–252.
- [25] J.J. McMahon, M. Barry, K.J. Breen, A.K. Radziwon, L.D. Brooks, M.R. Blair, Photocatalysis of the oxygen reduction reaction at adsorbate-covered silver, *J. Phys. Chem. C* 112 (2008) 1158–1166.
- [26] S. Barazzouk, P.V. Kamat, S. Hotchandani, Photoinduced electron transfer between chlorophyll A and gold nanoparticles, *J. Phys. Chem. B* 109 (2005) 716–723.